

Quasiperiodic Tip Splitting in Directional Solidification

B. Utter, R. Ragnarsson and E. Bodenschatz

Laboratory of Atomic and Solid State Physics, Cornell University, Ithaca, NY 14853

(October 28, 2018)

We report experimental results on the tip splitting dynamics of seaweed growth in directional solidification of succinonitrile alloys with poly(ethylene oxide) or acetone as solutes. The seaweed or dense branching morphology was selected by solidifying grains which are oriented close to the $\{111\}$ plane. Despite the random appearance of the growth, a quasiperiodic tip splitting morphology was observed in which the tip alternately splits to the left and to the right. The tip splitting frequency f was found to be related to the growth velocity V as a power law $f \propto V^{1.5}$. This finding is consistent with the predictions of a tip splitting model that is also presented. Small anisotropies are shown to lead to different kinds of seaweed morphologies.

PACS number(s): 68.70.+w, 81.30.Fb

Directional solidification of binary alloys has received considerable attention over the last fifty years as an example of a non-equilibrium pattern forming system with technological importance. A breakthrough in understanding was gained when surface tension anisotropy was identified as a singular perturbation that selects stable dendrites [1,2]. Many important experiments have been performed to understand the structure and dynamics of dendritic growth and great insights have been gained [3]. However, when growing a cubic crystal close to the $\{111\}$ plane, the surface tension is nearly isotropic and it was shown [4,5] that the growth is irregular with constant tip splitting. This is called seaweed growth [4], or dense branching morphology [6], and is also observed in such different systems as viscous fingering [7], bacterial colonies [8], electrodeposition [9], annealing magnetic films [10], and drying water films [11].

In this Letter, we report experimental results on the dynamics of seaweed growth in the directional solidification of binary succinonitrile alloys. By using a grain oriented near the $\{111\}$ plane, we observe quasiperiodic alternating tip splitting [5]. We find the tip splitting frequency to be related to the growth velocity by a power law with an exponent close to 1.5. We show that a simple model motivated by observations of the growth dynamics can explain this behavior and that a small misalignment of the crystal from the $\{111\}$ plane is necessary for quasiperiodic alternating tip splitting. To our knowledge, neither the scaling nor the regularly alternating splitting have been predicted theoretically. Our results show that different types of seaweed morphologies exist that at first sight would appear the same.

The surface tension anisotropy is based on the underlying cubic structure of the growing solid. Under typical conditions in low speed directional solidification, the orientation of the dendrites and sidebranches is determined by the crystalline structure, pulling direction, and imposed temperature gradient. Changing the angle between the crystalline axis and the pulling direction changes the

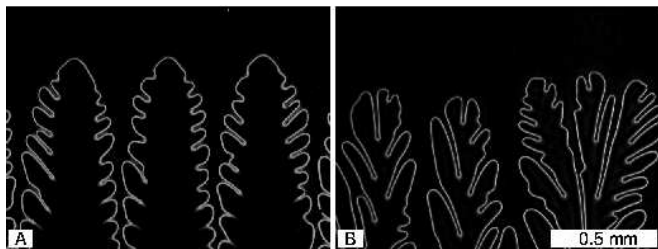


FIG. 1. Phase contrast micrographs of growth in directional solidification which differ only in crystalline orientation. (A) A dendrite (growth along $\{100\}$ direction) and (B) seaweed (near $\{111\}$ plane). The white line indicates the solid-liquid interface with the solid growing upwards into the undercooled melt. The thermal gradient (18 K/cm), concentration (0.25% PEO), and growth velocity V ($2.71 \mu\text{m/s}$) are the same.

degree and orientation of the effective anisotropy [5,12]. Because of the cubic symmetry, growth in the $\{111\}$ plane has an effective surface tension that is close to isotropic. As shown in Fig. 1, under the same growth conditions, dendrites are observed for crystals growing in the $\{100\}$ direction and disordered seaweeds with continuous tip splitting are observed for crystals oriented in the $\{111\}$ plane.

The present experiment was performed with a directional solidification apparatus in which a thin sample ($13\text{cm} \times 1.5\text{cm} \times (5-50)\mu\text{m}$) was moved through a linear temperature gradient at constant velocity [13]. In these experiments, the gradient was maintained at about 18 K/cm with a stability of ± 10 mK on each side. The two mixtures used were transparent alloys of 0.25% poly(ethylene oxide) (PEO) [14] and 1.5% acetone (ACE) in succinonitrile (SCN). The polymer has a very small partition coefficient and diffusivity ($k \approx 0.01$, $D \approx 80\mu\text{m}^2/\text{s}$) while for the acetone sample they are larger ($k \approx 0.33$, $D \approx 1300\mu\text{m}^2/\text{s}$) [15].

The solid-liquid interface is observed with phase contrast microscopy, and images are recorded using a CCD camera and time lapse video. To observe seaweed growth,

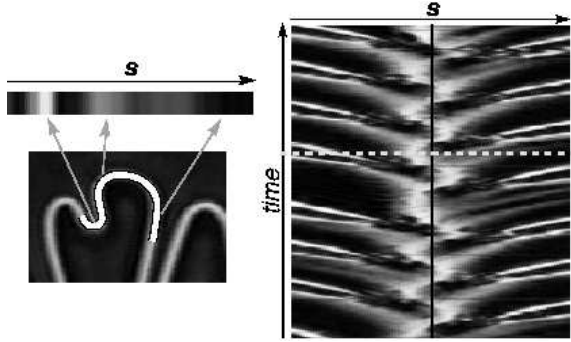


FIG. 2. Curvature-time (CT) plots for SCN-PEO. A representation of the curvatures along the interface near the tip. The solid-liquid interface is extracted and the absolute curvatures along a segment near the tip are plotted in greyscale. Sequences of these lines are stacked in time to create the plot on the right, where the center line represents the tip position. The tip segment highlighted on the left is indicated as a dashed line on the CT plot. White corresponds to high curvature (radius of curvature $< 10 \mu\text{m}$) and black to zero curvature. The time interval shown is 9.4 minutes and increases upwards. The width is $300 \mu\text{m}$ and $V = 2.71 \mu\text{m/s}$.

the sample is melted and quenched, seeding numerous grains. One grain with the optimal orientation is selected and all the others are melted off. The chosen grain is then allowed to grow and fill the width of the cell.

For seaweed growth, we observe two types of tip splitting events: (i) The tip splits off-center such that the larger of the two remaining tips continues to grow as the other falls behind. This can lead to growth in which the tip alternately splits towards the left and right at regular intervals as a single main branch steadily grows forward. (ii) The tip splits near its center producing two tips of comparable size. These two new branches interact with each other until either one falls behind, or they spread apart and grow as main branches. In this Letter, we will focus on the dominant case (i) and specifically on quasiperiodic alternating tip splitting.

We characterized the tip splitting process by measuring the curvature at each point along an arc centered on the tip, which we defined as the furthest point along the growth direction on a particular branch. The segment used is typically $300 \mu\text{m}$ long as compared to the tip radii of $(25-75)\mu\text{m}$. Plotting the curvature versus the position along the arc and stacking the plots from successive times, we created curvature-time (CT) plots as shown in Fig. 2. There, the greyscale intensity corresponds to the absolute value of the curvature. The striking feature is that the curvatures at the tip oscillate. The CT plot shows how the tip flattens and splits on one side before it begins to flatten on the other side. The bright pairs of lines to the sides represent the large curvature at the deep groove formed when a tip splits. The tip splitting is not random as one might expect for noise-induced splitting;

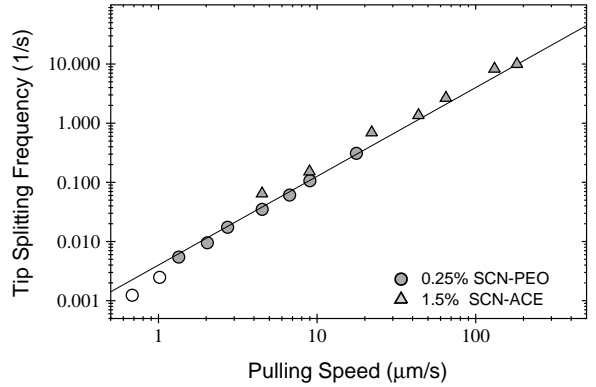


FIG. 3. Tip splitting frequency f versus growth velocity V for two samples. The solid line shows $f = 0.004 \times V^{1.5}$. The best fits for the individual runs give exponents of 1.56 ± 0.05 for SCN-PEO and 1.40 ± 0.05 for SCN-ACE. The two points below $1.1 \mu\text{m/s}$ were not used in the fit as they are below a transition to cellular growth as discussed later.

for most of the runs, the splitting alternates regularly for more than 85% of the time. It should be noted, however, that this behavior is quasiperiodic. The time between individual tip splittings fluctuates within 25% of the mean period and the tip occasionally splits multiple times on the same side.

The periodicity is also broken occasionally (typically after 10-20 cycles) when the tip splits nearly in the center, forming two symmetric main branches (case ii). These two “new” branches influence each other by initially suppressing the tip splitting on their adjacent sides, reminiscent of doublon growth [16]. Once one branch falls behind or the tips are separated sufficiently, the tips resume the quasiperiodic alternating tip splitting.

The splitting frequency was measured at each velocity by following a single branch over long times. It was determined from the peak of the power spectrum of the CT plot, from the peak of the probability distribution of time intervals between splitting events, or simply by counting the number of times the tip splits and dividing by the total time of the run, all of which gave the same results within measurement errors. As shown in Fig. 3, the splitting frequency as a function of velocity follows the power law $f \propto V^{1.5}$ for the two mixtures.

To model this behavior, we note that the tip flattens and widens before becoming unstable. One can expect that the wavelength λ_t of this tip instability is related to the initial instability of the flat interface λ_f under the same conditions. This is confirmed for both samples in Fig. 4 (inset). λ_t is smaller than λ_f since the expanding tip will split at the smallest wavelength that is unstable in this evolving state. Fig. 4 shows the wavelength λ_t as a function of pulling speed for both samples and the solid line corresponds to $\lambda \propto V^{-0.5}$. The exponent of $-\frac{1}{2}$ is the expected value for λ_f based on linear stability analysis [17]. In practice, λ_t is more convenient to measure since it

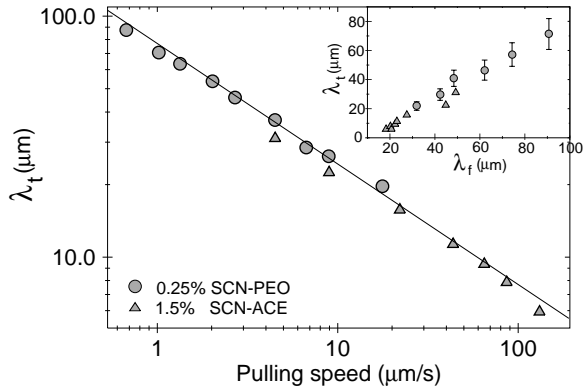


FIG. 4. The wavelength of the instability at the tip λ_t is plotted versus pulling speed. The line corresponds to $\lambda_t = 75 \times V^{-0.5}$. The measured power law exponents are -0.46 ± 0.05 for SCN-PEO and -0.48 ± 0.05 for SCN-ACE. The inset shows the approximately linear relationship between λ_t and λ_f . For SCN-PEO, $\lambda_t(V) = 0.85\lambda_f(V) - 7.4\mu\text{m}$ and for SCN-ACE, $\lambda_t(V) = 0.73\lambda_f(V) - 6.9\mu\text{m}$.

can be determined as an average over many events during the portion of the run being studied. From dimensional analysis, we now see that the frequency results from the pulling velocity V divided by the length scale λ . That is, $f \propto V/\lambda \propto V^{-3/2}$ appears to be satisfied.

Additional quantitative insight is gained by extracting the interface at subsequent times and superimposing the images to observe the growing solid (Fig. 5A). It is apparent that the flat region of the tip grows until it is wide enough to become unstable. We observe that the tip widens at a constant rate until it reaches the instability length of the initial flat interface. After splitting, the surviving tip widens in a similar way. As seen in Fig. 5B, we can view this process as a series of triangles formed by the flat regions. For SCN-PEO, we often observe a delay between consecutive splittings, which introduces a gap between the triangles in Fig. 5B. This may be explained by the fact that the tip is initially constrained by the presence of the neighboring tip and is inhibited from widening until the neighbor falls behind. The average period between splitting is $\tau = 1/f$ and we assume the delay time is a fixed fraction of the average period, $\tau_d = \alpha\tau$, where α is constant for a given sample. If α is small, the angle θ at which the tip widens is predicted from Fig. 5C to be

$$\theta_{th} = 2 \arctan \left(\frac{\lambda_f f}{2V} (1 + \alpha) \right). \quad (1)$$

All quantities on the right, other than the free parameter α , have been measured, so a quantitative comparison can be made between the predicted value θ_{th} and θ_{ex} which was measured directly from the experimental pictures. Fig. 6 presents this data for the two mixtures considered. We observed excellent agreement between the model and the measurement. In addition, we observe

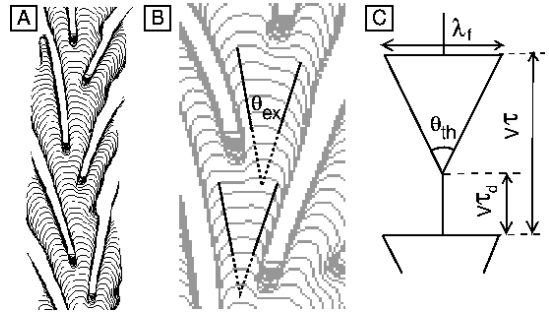


FIG. 5. (A) The interface is extracted at sequential times and superimposed to observe the growing tip. (B) An approximately flat region of the tip is seen to grow linearly in time. The boundaries of this expanding flat region (solid lines) are traced back (dashed) to the same point. (C) Schematic of the growth process (see text).

the angle to be independent of velocity, which with Eq. 1 implies the above scaling relationship, $f \propto V/\lambda$. It also suggests that θ depends only on a materials property, such as the surface tension of the growing solid. The fact that the two samples show similar angles may indicate that a similar surface tension profile exists in these particular grains. The drop off at low speeds for SCN-PEO reflects a change in morphology since when the speed was decreased the growth became increasingly cellular and the tip did not continually split. It is unclear why the SCN-ACE sample does not exhibit the delay seen in the SCN-PEO mixture.

The above observations suggest that the alternating tip splitting may be correlated with specific crystalline orientations near $\{111\}$ and not with the choice of solute or sample dimensions. In fact, Akamatsu et al. also noted a region of quasiperiodicity in a $\text{CBr}_4\text{-C}_2\text{Cl}_6$ mixture which is similar to our observations [5]. It is important to note that it is possible to seed other kinds of seaweeds in these samples which do not exhibit this striking periodicity. This confirms that the specific grain is important.

To support this conjecture, the temperature gradient was decreased in order to diminish the effect of the imposed growth direction. Fig. 7 compares a space-time plot (ST) [18] of a quasiperiodic tip splitting growth (Fig. 7A) with that for the same grain when the temperature gradient is decreased (Fig. 7B). The growth locks into two symmetric directions revealing the weak anisotropy. This accounts for the tendency of the tip to grow outward and flatten as growth along these directions is preferred. After converting time into distance, the angle between the two growth directions in Fig. 7B is 40° , which should be an upper limit on the angle measured in Fig. 6. We conclude that a small amount of anisotropy has important consequences on the seaweed growth observed. It also confirms that seaweed growth is possible for weak anisotropy.

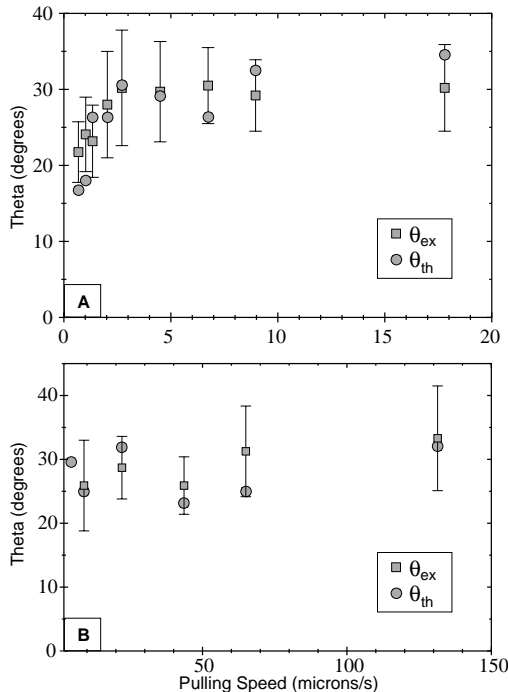


FIG. 6. Comparison of the measured and predicted angles θ_{ex} and θ_{th} . (A) SCN-PEO with $\alpha = 0.37$ and (B) SCN-ACE with $\alpha = 0$.

In conclusion, experimental studies of the low anisotropy seaweed growth morphology for certain grains show surprisingly regular tip splitting despite its generally disordered appearance. We find that the curvature of the tip oscillates, reflecting the cyclic changes in its shape which lead to alternating tip splitting. The tip splits quasiperiodically, with a frequency that is related to the growth velocity as $f \propto V^{3/2}$. We present a simple model that assumes that the tip splits when the width of the flat region on the tip is sufficiently wide for the linear instability to occur. The angle at which the tip widens is independent of growth velocity explaining the observed scaling relation. We show evidence that a slight anisotropy in the surface tension causes the observed alternating tip splitting. It is interesting to ask whether the behavior observed here could also be found in other systems, such as Saffman-Taylor fingering where a weak anisotropy is imposed.

We thank Nigel Goldenfeld for valuable discussions. This work was supported by the Cornell Center for Materials Research (CCMR), a Materials Research Science and Engineering Center of the National Science Foundation (DMR-0079992).

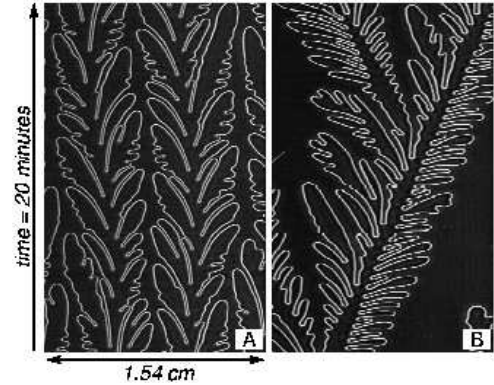


FIG. 7. Space-time (ST) plot of a single grain growing at $2.71 \mu\text{m/s}$. (A) The quasiperiodic splitting is observed, but when the temperature gradient is decreased from 18K/cm to (B) 3K/cm , the degeneracy of growth is revealed as the growing solid locks into two symmetric directions. The total time shown is 20 minutes in both pictures.

- [1] D. Kessler, J. Koplik, and H. Levine, *Physical Review A* **31**, 1712 (1985).
- [2] E. Ben-Jacob, N. Goldenfeld, B. Kotliar, and J. Langer, *Physical Review Letters* **53**, 2110 (1984).
- [3] W. Kurz and R. Trivedi, *Acta Metall. Mater.* **38**, 1 (1990).
- [4] T. Ihle and H. Müller-Krumbhaar, *Phys. Rev. Lett.*, **70**, 3083 (1993), *Phys. Rev. E*, **49**, 2972 (1994).
- [5] S. Akamatsu, G. Faivre, and T. Ihle, *Phys. Rev. E*, **51**, 4751 (1995). In particular, note Fig. 20 which highlights a region of quasiperiodicity similar to these results.
- [6] E. Ben-Jacob *et al.*, *Phys. Rev. Lett.* **57**, 1903 (1986).
- [7] K. McCloud and J. Maher, *Phys. Rep.* **260**, 139 (1995).
- [8] T. Matsuyama and M. Matsushita, *Crit. Rev. Microbiol.* **19**, 117 (1993).
- [9] O. Zik and E. Moses, *Physical Review E* **53**, 1760 (1996).
- [10] C. H. Shang, *Physical Review B* **53**, 13759 (1996).
- [11] N. Samid-Merzel, S. Lipson, and D. Tannhauser, *Physica A* **257**, 413 (1998).
- [12] S. Akamatsu and G. Faivre, *Phys. Rev. E* **58**, 3302 (1998).
- [13] R. Ragnarsson, B. Utter, and E. Bodenschatz, in *Phase Transformations and Systems Driven Far From Equilibrium*, edited by E. Ma (Materials Research Society, Warrendale, PA, 1998), Vol. 481, pp. 65–70.
- [14] Poly(ethylene oxide) with an attached rhodamine dye (Sulferhodamine Bis-(PEG 2000), molecular wt. 4500) is purchased from Molecular Probes, Inc. (Eugene, OR).
- [15] M. Chopra, M. Glicksman, and N. Singh, *Metallurgical Transactions A* **19A**, 3087 (1988).
- [16] E. Brener *et al.*, *Physica A* **204**, 96 (1994).
- [17] W. W. Mullins and R. F. Sekerka, *Journal of Applied Physics* **35**, 444 (1964).
- [18] For an explanation of ST plots see, for example, [12].